MATERIALS PHYSICS AND MECHANICS RESEARCH ARTICLE

Submitted: September 11, 2025 **Revised: October 29, 2025** **Accepted: December 4, 2025**

The elastic properties of natural fibre reinforced composite materials using homogenisation modeling

R.E. Guzman-Lopez [1], S. Gomez Suarez [1], R.A. Gonzalez-Lezcano [2]

[1] Universidad Pontificia Bolivariana, Bucaramanga, Colombia

[2] Universidad San Pablo-CEU, Madrid, Spain

rgonzalezcano@ceu.es

ABSTRACT

The numerical simulation of composite materials brings in a challenge in the resolution of problems with a high nonlinearity of both, material, and geometry (geometrically complex structures), with different size scales. Some common examples such as additive manufacturing 3D, metal alloys, porous media, polycrystalline materials and composites, a significant computing challenge is shown where all length scales are resolved by a single finite element model. This would require many elements, and computing the solution would be unfeasible, even using modern and near-future computing resources. The standard way to solve this situation of scale in finite element analysis is numerical homogenization technique. Material properties for a composite material are average, instead of simulating the full microstructure. With homogenized material data, it only required a macroscopic simulation using significantly less computational sources. The mechanical behavior of composites materials reinforced with natural fibers, is studied by means of a short fiber composite numerical model. The influence that the spatial distribution and the volumetric fraction of the cylindrical fibers have on the effective elastic properties of the numerical model was established (Young´s modulus *E*, Shear modulus *G*, Poisson´s ratio) - curves are presented corresponding to tension test applied on fique fibers and polylactic acid-biopolymer.

KEYWORDS

representative volume element • multiparticle cell • fiber-reinforced composites • composite materials natural fibre composites

Funding. *The authors would like to express their gratitude to Engineering Department of Universidad Pontificia Bolivariana-Bucaramanga, project code: BIC-008-0822-F4M.*

Citation: Guzman-Lopez RE, Gomez Suarez S, Gonzalez-Lezcano RA. The elastic properties of natural fibre reinforced composite materials using homogenisation modeling. *Materials Physics and Mechanics*. 2026;54(1): 130–138. http://dx.doi.org/10.18149/MPM.5412026_12

Introduction

The usage of methods and models to evaluate thermo-elastic properties of composite materials has been widely investigated in the past years. Different models have been proposed and are currently used in many engineering applications, including analytical models [1–6], semi-empirical models [7–9], homogenization models [8,10,11] and cell methods [12–15]. The cell models are generally constructed from a discretization by the finite element method (FEM) of a representative volume element (RVE) of a composite material. Obtaining RVE can generally be done using numerical algorithms [9,10] and it must be a volume small enough from a macroscopic point of view to be treated as a continuous point of matter and, at the same time, large enough to be considered representative of the meso/micro-structure of the material.

The analytical models are based on the fact that the effective mechanical properties of the composite can be obtained by relations between the volumetric measure of the meso/micro stress and strain fields. In the elastic regime, the analytical models represent the stress and strain fields present in the composite material through their average values in matrix and reinforcement. The individual contributions are quantified considering that the average stresses and strain in each phase are related through their respective stiffness tensors, C_m and C_i. The objective of the analytical models (meanfield) in elasticity is centered by finding the stiffness tensor [C] of the elastic constitutive matrix $\bar{\sigma} = C : \bar{\varepsilon}$. Mori-Tanaka [10] developed a well-known model which is widely used for modeling different kinds of composite materials, based on the studies of Eshelby [4] and Benveniste [11] of tensional fields inside a particle embedded in an elastic matrix of infinite length, based on an Equivalent inclusion method. In [16], it was suggested self-consistent formulation in which the material is represented in such a way that all phases are embedded in an equivalent material whose properties are the properties to be determined. Christensen et al. [17] also proposed their generalized self-consistent formulation, in which the particle is embedded in a matrix, and this particle–matrix composite, in turn, is embedded in a material whose elastic constants are the unknowns of the problem. Whitney and Riley [18] proposed analytical expressions using strain-energy balances to obtain elastic constants in composite materials reinforced with unidirectional fibers.

FEM has been extensively used in the literature to analyze a periodic unit cell, to determine the thermo-mechanical properties and damage mechanisms of composites [14,18]. Böhm H. [19] studied unit cell models for describing the elastoplastic behavior of short fiber reinforced metal matrix composites (MMCs) reinforced by randomly oriented short fibers, providing a foundational approach for micro-scale modeling.

Zihui Xia et al. [20] presented a FEM micromechanical analysis method applied to unidirectional and angleply laminates subject to multiaxial loading conditions, demonstrating the application of FEM in varied reinforcement configurations. Younes R. [21] presented a comparative study of analytical micromechanical models and numerical models (FEM) evaluating the elastic properties of unidirectional composite materials (glass/epoxy, carbon/epoxy, polyethylene/epoxy composite), offering critical insight into the validity of numerical models. Srivastava V.K. [22] used numerical homogenization tools for the evaluation of the effective material properties of the short fiber composites, using modified random sequential adsorption algorithm (RSA) [22,23], which is a relevant approach for generating realistic microstructures.

The homogenization method based on the finite element method (FEM) allows the replacement of a heterogeneous medium with an equivalent homogeneous one using information from the meso/micro scale, through the local response, on the microscopic scale depending on the state of charge on the macro scale. In cell models, the macroscopic stress and strain tensors associated with a particular mechanical stress imposed on the multiparticle cell can be obtained in two ways: They may be calculated either from the external forces acting on the faces of the cell or from the volumetric average of the stress and strain microfields within the calculation domain [13,24–27].

The homogenization method establishes mathematical relationships between the meso/micro fields and the macroscopic stress–strain fields by using cell-based formulations derived from perturbation theory. In homogenization models for short-fiber

composite materials, it is generally recommended to employ representative volume elements (RVEs) that contain a sufficiently large number of fibers to capture the statistical characteristics of their spatial distribution.

One common approach to determine an appropriate RVE size consists of selecting an initial RVE and performing macroscopic simulations to assess the influence of fiber spatial arrangement on stress and strain fields. The size of RVE is then progressively increased to verify whether the microscopic results change significantly. If notable variations occur, the initial RVE size is insufficient; if results remain stable, the initial RVE can be considered representative.

In this work, the geometries and meshes of RVEs were generated using Ansys Material Designer 2024R1, whose algorithms compute the homogenized properties of a composite from the known properties of its constituent materials. The developed Short Fiber Composite Model (RVE) was used to analyze the influence of model parameters—such as fiber volume fraction (*f*) and fiber orientation—on the resulting homogenized elastic properties (Young's modulus *E*, shear modulus *G*, and Poisson's ratio *v*).

Furthermore, as requested, a more detailed analysis of the key publications cited in this section has been incorporated, highlighting their methodological contributions and relevance to the present homogenization framework.

Methods

Characteristics of the RVE model

The micromechanical model for the composite material reinforced with fique fibers is configured using the RVE technique. The model is characterized by several parameters that define the geometry and distribution of fibers within the RVE. These parameters include the fiber volume fraction, which represents the portion of the RVE occupied by the fiber material, and the seed number used to generate random fiber orientations in the case of randomized RVEs. The model also incorporates the orientation tensor, the aspect ratio (defined as the ratio of fiber length to diameter), and the total number of cylindrical fibers contained in the RVE.

As shown in Fig. 1, the RVE model of the composite material consists of short fique fibers randomly arranged in a polylactic acid (PLA) biopolymer matrix. The cylindrical reinforcement fibers are generated without spatial interference, and if a fiber intersects one of the planes that defines the boundaries of the cell, it is duplicated on the opposite face of the cell. This procedure results in a multiparticle cell with periodic geometry (Fig. 1). The generated RVE was used to analyze the influence of the fiber volume fraction and fiber orientation (*f*) on the engineering constants E_x, E_y, E_z, G_{xy}, G_{yz}, G_{xz}, ν_{xy}, ν_{yz}, and ν_{xz}.

The orientation is randomly assigned by tracing a symmetric orientation tensor. The tensor A and its components Aij are now expressed consistently using italic mathematical notation to ensure uniformity throughout the manuscript. The three diagonal entries are: A_{11}, A_{22}, and A_{33}. These values indicate how closely the fibers are aligned with the corresponding coordinate direction. In this case, multiparticle models were generated in which the fibers are oriented parallel to the XZ plane:

$$A_{i,j} = \sum_{k=1}^{N} {d_i}^{(k)} {d_j}^{(k)}. \quad (1)$$

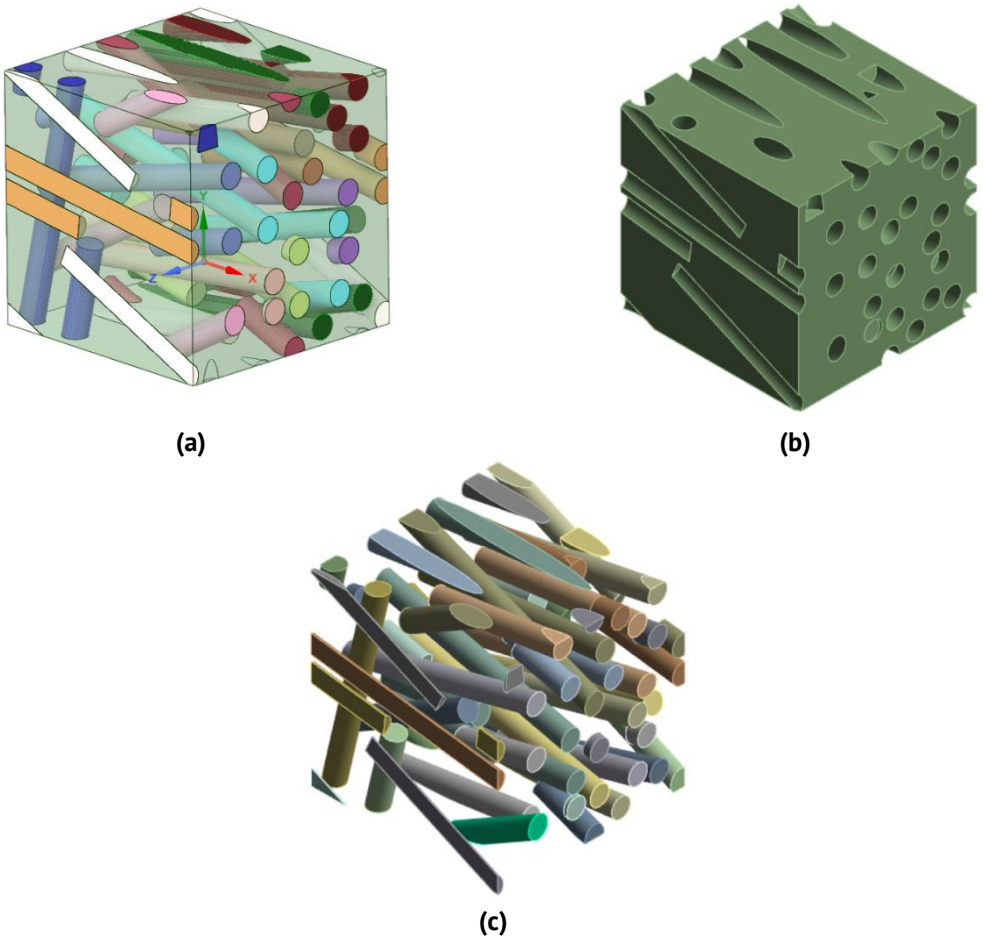

Fig. 1. Parts of the RVE: (a) composite NFCs, (b) matrix, (c) short fibers

Numerical FE modeling

The geometries and periodic meshes of the RVE were generated using Ansys Material Designer 2024 R1. Figure 2 shows the distributed mesh-quality metric for the model, which was discretized using 4-node tetrahedral elements. This metric is based on the ratio between the element volume and the square root of the cube of the sum of the squared edge lengths for 3D elements. As a general rule, the minimum acceptable value for this mesh metric should be greater than 0.2.

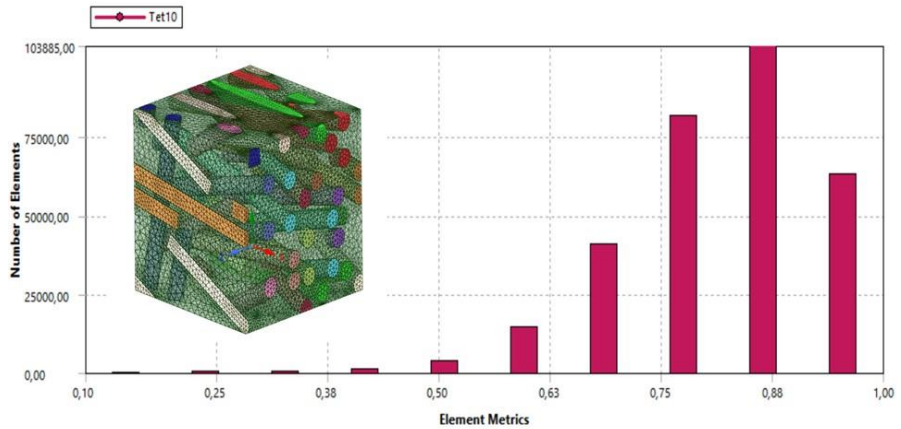

Fig. 2. The mesh-quality metric for the model RVE

For the model shown in Fig. 2, the mesh consists of 309,319 elements and 434,508 nodes. The generation parameters used were: fiber volume fraction $f = 0.1$, number of fibers $N = 24$, aspect ratio = 15, and orientation tensor components $A_{11} = 0$, $A_{22} = 0.8$ and $A_{33} = 0.2$ indicating that the fibers are oriented parallel to the XZ plane.

Results

The mechanical properties of the constituent materials used in the numerical multiparticle-cell models were obtained from tensile tests performed on the fique fibers and the PLA matrix (Ingeo biopolymer 2003D). Figure 3 shows the stress–strain (σ–ε) curves corresponding to the tensile tests conducted on both the fique fibers and the polylactide (PLA) matrix. The σ–ε curves are plotted up to the respective tensile ultimate strenghts.

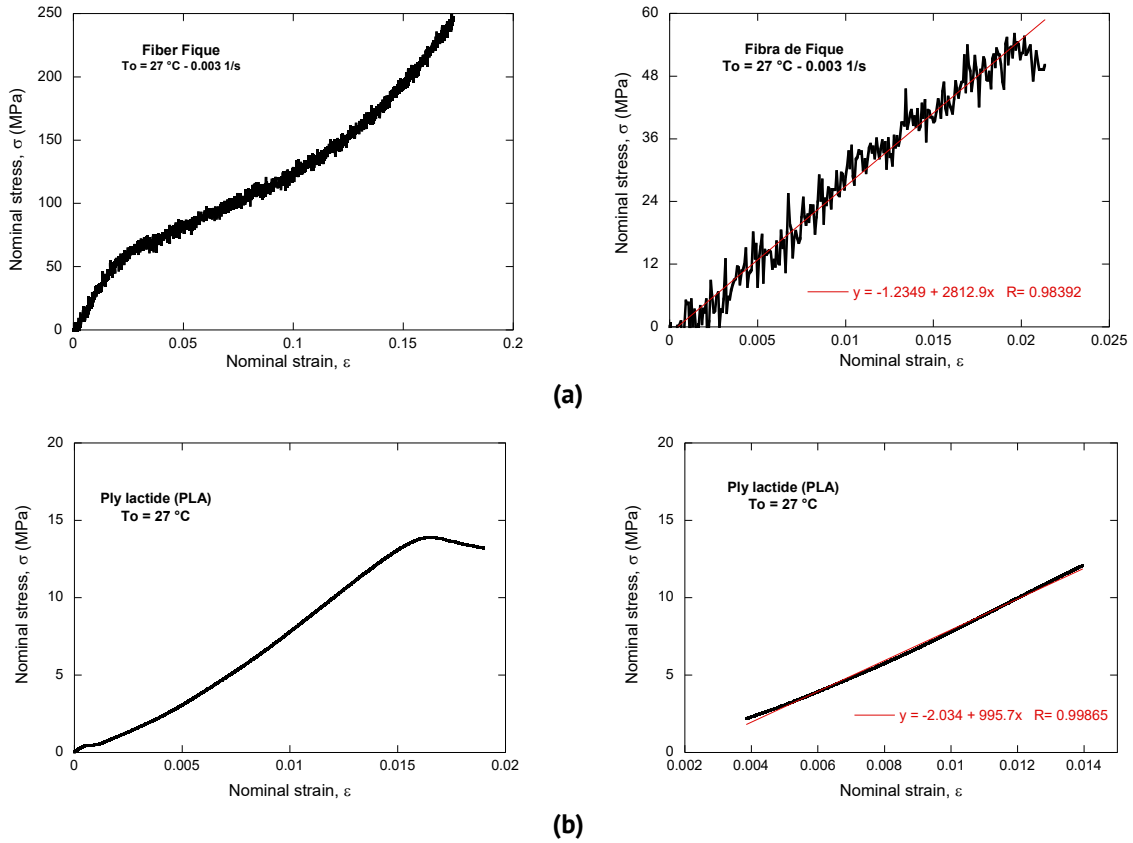

Fig. 3. (a) Stress–strain (σ–ε) curves obtained experimentally for the polylactide (PLA) matrix at 27 °C, including the complete response up to the ultimate tensile strength and the linear fit in the elastic region. (b) Stress–strain (σ–ε) curves for the fique fibers tested at 27 °C and a strain rate of 0.003 s^{-1}, showing the full mechanical response and the corresponding linear fit in the elastic region. The equations of the fitted lines and the correlation coefficient R are included in each graph

Table 1 displays elastic modulus, the poisson´s ratio and the tensile ultimate strength of the materials that are used in the RVE model. The geometric parameters of diameter D, and aspect ratio (L/D) of the short fibers of the RVE model are presented in Fig. 4. The normal distribution curves are shown, being able to set a mean value and its standard deviation for 198 measured values. Figure 5 shows the cross section of a fiber and the lengths of some short fibers can be observed.

Table 1. Material properties for the constituents of the composite

Materials	Elastic modulus, GPa	Poisson's ratio	Tensile ultimate strength, MPa
Fique	0.943–2.800	0.300	30.000–240.000
PLA	0.995	0.360	13.900

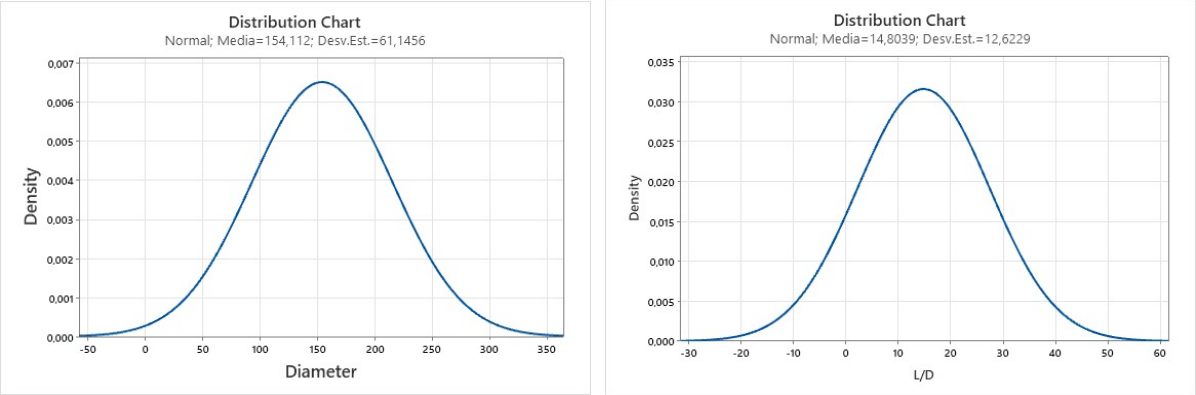

(a) **(b)**

Fig. 4. (a) Chart distribution normal of values the fiber diameter and (b) aspect ratio

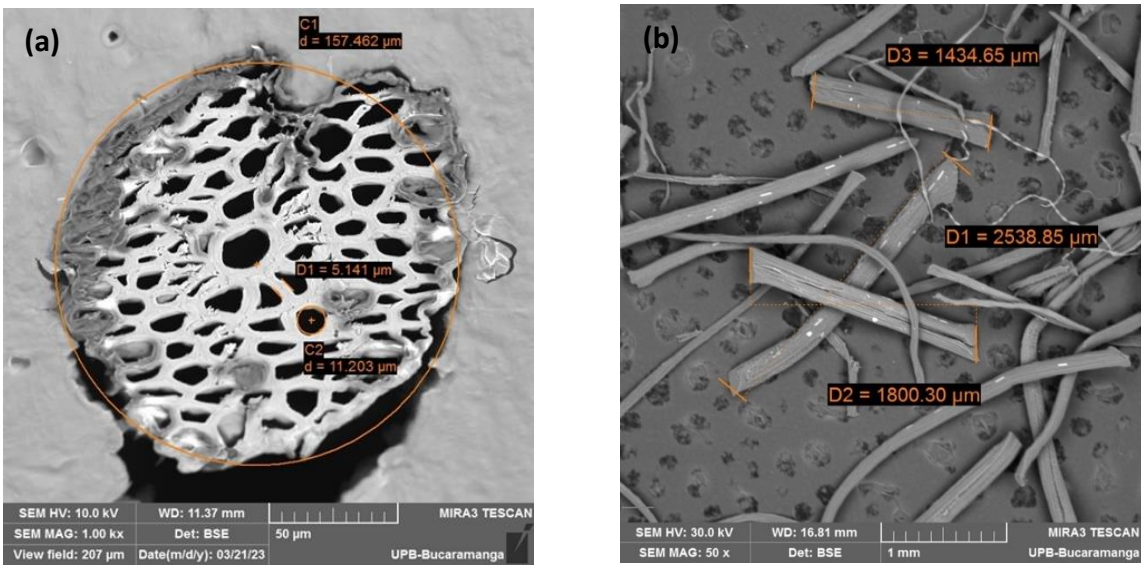

Fig. 5. (a) Cross section of raw fique fibers, SEM image: 1000 x magnification. (b) Longitudinal image of raw fique fibers magnified at 50

Table 2 shows the results of the FEM analysis of the elastic engineering constants for several RVE models. The dependence of the results with respect to the fiber volume fraction and the tensor orientation is observed, keeping the aspect ratio ($L/D \approx 15$) constant. Figure 6 shows the results of the elastic modulus in the directions E_x, E_y, E_z, and the shear moduli G_{xy}, G_{yz}, G_{zx}, as expected, they increase with the volumetric fraction, while ν is decreasing, it is also observed that the variation of the orientation of the fibers given by the orientation tensor ($A_{i,j}$) are not significant (Table 2). According to the fact that the random distribution of the fibers is parallel to the XZ plane, the results present an isotropic behavior in the plane, while the perpendicular components present significant differences.

Table 2. Numerical results for elastic engineering constants

Parameters	Value #1	Value #2	Value #3	Value #4	Value #5	Value #6	Value #7
Fiber volume fraction	0.05145846	0.051468	0.102659	0.102723	0.193572	0.205736071	0.244535
Orientation tensor A_{11}	0.2000062	0.299994	0.22155	0.3627	0.223056	0.332688133	0.269775
Orientation tensor A_{22}	0.7999938	0.700006	0.77845	0.6373	0.776944	0.667311867	0.730225
Number of fiber	34	34	24	24	16	17	11
Engineering constants							
E_1, MPa	1048.04669	1050.762	1103.798	1109.172	1224.381	1230.306896	1281.017
E_2, MPa	1069.42596	1065.035	1140.699	1127.192	1288.706	1274.770353	1349.442
E_3, MPa	1047.52113	1047.6	1102.763	1103.917	1208.46	1223.474354	1274.172
G_{12}, MPa	38.112641	388.3994	412.3265	413.9153	451.792	465.2257714	481.4119
G_{23}, MPa	385.002686	384.913	404.9138	404.6695	442.8969	448.8552857	467.5487
G_{31}, MPa	383.727959	383.9225	402.775	403.0845	438.1448	445.3709344	461.6207
n^{12}	0.35082724	0.352427	0.344875	0.350177	0,328909	0.339509741	0.330379
n^{13}	0.36139787	0.360252	0.360531	0,356824	0.361243	0.354052931	0.355162
n^{23}	0.35626227	0.356909	0.352371	0.353002	0.349525	0.345615269	0.343473
Density							
$r^{(t\ mm\text{^}-3)}$	3.13E-09	3.13E-09	3.13E-09	2.86E-09	2.86E-09	2.86E-09	2.79E-09

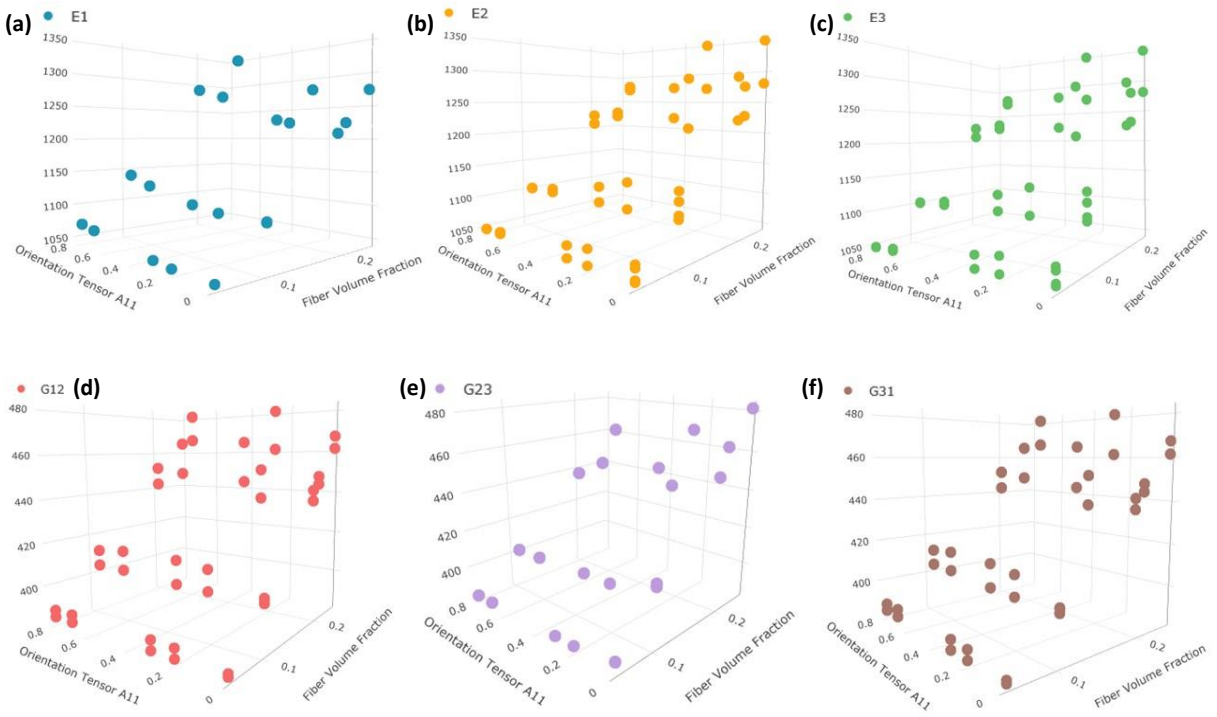

Fig. 6. (a–c) Elastic moduli E_x, E_y, E_z and (d–f) shear moduli G_{12}, G_{23}, G_{31}

Conclusions

1. Influence of fiber volume fraction: the elastic properties of the natural fiber composites (NFCs) increase consistently with higher fiber volume fractions. This confirms that the reinforcing effect of fique fibers is directly proportional to their concentration within the PLA matrix.
2. Effect of fiber orientation: for the RVEs generated in this study—where fibers were intentionally aligned parallel to the XZ plane—significant directional dependence was observed in the elastic moduli (E_x, E_y, E_z), shear moduli (G_{xy}, G_{yz}, G_{xz}), and Poisson ratios (ν_{xy}, ν_{yz}, ν_{xz}). Mechanical anisotropy arises predominantly from this controlled orientation.
3. Spatial distribution of fibers: although extrusion processes typically lead to non-uniform particle distribution due to flow-induced alignment or clustering, the numerical results obtained here indicate low sensitivity of effective elastic properties to the particular fiber distributions examined. This outcome may be related to the restricted set of configurations analyzed.
4. Agreement between transverse and longitudinal moduli: for a given fiber volume fraction, the elastic modulus showed a tendency toward similar values along the transverse and longitudinal directions, except in the direction perpendicular to the XZ plane, where fiber alignment dominates mechanical behavior.
5. General mechanical response of the composite: the combined effects of fiber volume fraction, spatial distribution, and orientation determine the global stiffness of NFCs. Among these factors, fiber orientation is shown to be the most decisive in governing anisotropy, while fiber distribution plays a comparatively minor role within the analyzed parameter space.

CRediT authorship contribution statement

Rolando Enrique Guzman-Lopez: conceptualization, methodology, investigation, writing—original draft preparation, writing—review and editing, supervision, project administration; **Sergio Gomez Suarez**: conceptualization, methodology, investigation, writing—original draft preparation, writing—review and editing; **Roberto Alonso Gonzalez-Lezcano**: methodology, investigation, writing—review and editing, supervision.

Conflict of interest

The authors declare that they have no conflict of interest.

References

1. Voigt W. On the relationship between the two elastic constants of an isotropic body. *Ann. Phys.* 1889;274(12): 573–587.
2. Reuss A. Berechnung der Fließgrenze von Mischkristallen auf Grund der Plastizitätsbedingung für Einkristalle. *ZAMM - J. Appl. Math. Mech.* 1929;9(1): 49–58.
3. Hashin Z, Rosen BW. The Elastic Moduli of Fiber-Reinforced Materials. *J. Appl. Mech.* 1964;63: 223–232.
4. Eshelby JD. The determination of the elastic field of an ellipsoidal inclusion, and related problems. *Proc. Roy. Soc. A.* 1957;241(1226): 376–396.

5. Theocaris PS, Spathis G, Sideridis E. Elastic and viscoelastic properties of fibre-reinforced composite materials. *Fibre Sci. Technol.* 1982;17(3): 169–181.
6. Whitney JM, Riley MB. Elastic properties of fiber reinforced composite materials. *AIAA J.* 1966;4(9): 1537–1542.
7. Affdl JCH, Kardos JL. The Halpin-Tsai equations: A review. *Polym. Eng. Sci.* 1976;16(5): 344–352.
8. Hill R. Theory of mechanical properties of fibre-strengthened materials: I. Elastic Behaviour. *J. Mech. Phys. Solids.* 1965;13(4): 189–198.
9. Chamis CC. Mechanics of composite materials: Past, present, and future. *J. Compos. Technol. Res.* 1989;11(1): 3–14.
10. Mori T, Tanaka K. Average stress in matrix and average elastic energy of materials with misfitting inclusions. *Acta Metall.* 1973;21(5): 571–574.
11. Benveniste Y. A new approach to the application of Mori-Tanaka's theory in composite materials. *Mech. Mater.* 1987;6(2): 147–157.
12. Millithaler P., Sadoulet-Reboul E., Ouisse M., Dupont J. B., Bouhaddi N. Equivalent orthotropic material properties for stators of electric cars. *Civil-Comp Proc.* 2015;106: 1–12.
13. Rodríguez FJ, Dardati PM, Godoy LA, Celentano DJ. Derivation of nodular cast iron elastic properties via computational micromechanics. *Rev. Int. Metod. Numer. Para Calc. y Disen. En Ing.* 2015;31(2): 91–105.
14. Viñuela JZ, Torres M, Silva RG. Cohesive zone modeling in load – unload situations. *Int. J. Mech. Sci.* 2022;222: 107205.
15. Rodriguez FJ, Dardati PM, Godoy LA, Celentano DJ. A computational micromechanics approach to evaluate effective properties of ductile cast iron. In: *Proc. 10th Int. Symp. Sci. Process. Cast Iron – SPCI10 A, 2014*. 2014.
16. Den Eindmck V. *Berechnung der elastischen Konstanten des Vielkristalls aus den Konstanten des Einkristalls.* 1958.
17. Christensen RM, Lo KN. Solutions for effective shear properties in three phase sphere and cylinder models. *Journal of the Mechanics and Physics of Solids*. 1979;27(4): 315–330.
18. Hyer MW, Waas AM. Micromechanics of Linear Elastic Continuous Fiber Composites. In: *Compr. Compos. Mater.* 2000. p.345–375.
19. Böhm HJ, Eckschlager A, Han W. Multi-inclusion unit cell models for metal matrix composites with randomly oriented discontinuous reinforcements. *Comput. Mater. Sci.* 2002;25(1–2): 42–53.
20. Xia Z, Zhang Y, Ellyin F. A unified periodical boundary conditions for representative volume elements of composites and applications. *Int. J. Solids Struct.* 2003;40(8): 1907–1921.
21. Younes R, Hallal A, Fardoun F, Hajj F. Comparative Review Study on Elastic Properties Modeling for Unidirectional Composite Materials. In: Hu N. (Ed.) *Compos. Their Prop.* 2012. p.1–18.
22. Srivastava VK, Gabbert U, Berger H. Representative volume element analysis for the evaluation of effective material properties of fiber and particle loaded composites with different shaped inclusions. In: Proulx T. (Ed.) *Mechanics of Time-Dependent Materials and Processes in Conventional and Multifunctional Materials, Volume 3. Conference Proceedings of the Society for Experimental Mechanics Series.* New York: Springer; 2011. p.185–192.
23. Kari S. *Micromechanical modelling and numerical homogenization of fibre and particle reinforced composites.* Germany; 2007.
24. Zahr-Viñuela J. *Comportamiento mecánico de materiales compuestos de matriz metálica y refuerzo de partículas : un enfoque basado en celdas multipartícula.* 2010.
25. García Sánchez GF, Guzmán López RE, Gonzalez-Lezcano RA. Fique as a sustainable material and thermal insulation for buildings: study of its decomposition and thermal conductivity. *Sustainability.* 2021;13(13): 7484.
26. Pavan R, Prashant A, Ameen T, Yashwant M, Avinash S, Irulappasamy S. Numerical simulation of low-velocity impact test on biocomposite laminates. *Materials Physics and Mechanics.* 2022;50(4): 355–364.
27. Suardana NPG, Lokantara IP, Lim JK. Influence of water absorption on mechanical properties of coconut coir fiber/poly-lactic acid biocomposites. *Materials Physics and Mechanics.* 2011;12(1): 45–53.